

An alternative approach to the tomographic reconstruction of smooth refractive index distributions

E. de la Rosa-Miranda

Unidad Académica de Ingeniería Eléctrica, Universidad Autónoma de Zacatecas, Antiguo Camino a la Bufa No. 1, Col. Centro. C. P. 98000, Zacatecas, Zac. México

L. R. Berriel-Valdos
berval@inaoep.mx

Luis Enrique Erro No. 1, Santa María Tonantzintla, San Andrés Cholula, C.P. 72840, Puebla, México

E. Gonzalez-Ramirez
gonzalez_efren@hotmail.com

Unidad Académica de Ingeniería Eléctrica, Universidad Autónoma de Zacatecas, Antiguo Camino a la Bufa No. 1, Col. Centro. C. P. 98000, Zacatecas, Zac. México

D. Alaniz-Lumbreras

Unidad Académica de Ingeniería Eléctrica, Universidad Autónoma de Zacatecas, Antiguo Camino a la Bufa No. 1, Col. Centro. C. P. 98000, Zacatecas, Zac. México

T. Saucedo-Anaya
tsaucedo@fisica.uaz.edu.mx

Unidad Académica de Física, Universidad Autónoma de Zacatecas, Calzada Solidaridad Esquina con Paseo a la Bufa S\N. Col. Centro. C. P. 98000, Zacatecas, Zac. México

J. I. de la Rosa-Vargas
ismaelrv@yahoo.com

Unidad Académica de Ingeniería Eléctrica, Universidad Autónoma de Zacatecas, Antiguo Camino a la Bufa No. 1, Col. Centro. C. P. 98000, Zacatecas, Zac. México

J. J. Villa-Hernández
jvillah@yahoo.com

Unidad Académica de Ingeniería Eléctrica, Universidad Autónoma de Zacatecas, Antiguo Camino a la Bufa No. 1, Col. Centro. C. P. 98000, Zacatecas, Zac. México

V. Torres-Argüelles

Instituto de Ingeniería, Universidad Autónoma de Ciudad Juárez, Av. del Charro 450 Norte, C.P. 32310, Ciudad Juárez, Chihuahua, México

V. M. Castaño

Centro de Física Aplicada y Tecnología Avanzada, Universidad Nacional Autónoma de México, Campus Juriquilla, Querétaro, Querétaro, México (On sabbatical leave at Universidad Autónoma de Querétaro)

Continuous, mathematically smooth Phase Objects with radial symmetry are reconstructed from cross sections of their refractive index distribution by a novel method, consisting of a linear combination of Gaussian basis functions, whose technical details are discussed. As an application example, this approach is used to get a fast and accurate estimation of the temperature distribution of an actual soldering tip. [DOI: <http://dx.doi.org/10.2971/jeos.2013.13036>]

Keywords: Optical tomography, phase object, metrology, interferometry

1 INTRODUCTION

Optical tomography is a well known nondestructive and non-invasive technique for obtaining the distribution of refractive index gradients in a cross section of a Phase-Object (PO), in the non-refractive limit, from one or more projections. In the case of a radially-symmetrical PO, only one projection is necessary [1]. This projection is formed by a set of parallel rays known as summa rays (Figure 1). For reconstructing a cross-section of a PO from their projections, back projections methods or Algebraic Reconstruction Technique (ART) [2]–[5] is normally employed.

Some other authors propose, alternatively, a reconstruction method by using Gaussian basis functions, solved by a regularization process [6]. In algebraic methods, the diagram of projections is a linear transformation of the cross section of the object to be reconstructed, i.e. a linear system given by the matrix of projections. Thus, the unknown vector consists of the image of the cross section and the solution vector of the diagram of projections [2]–[5]. From a technological standpoint, however, one of the main practical limitations of this otherwise powerful optical technique is the required computing

time to be able to extract meaningful information for on-line applications and a great effort has been then dedicated to that purpose. Accordingly, in this work we present a fast numeric estimation of refractive smooth index from an interferogram without the need of a carrier, by using non-local Gaussian basis functions. A comparison of our method and a traditional procedure is also included, as well as an actual example of the application of this technology to the optical determination of the temperature distributions around a soldering tip.

2 THEORETICAL BACKGROUND

Interferometric techniques are routinely used to measure a number of physical quantities [1, 7], such as temperature, pressure or strain, provided they can be associated to the distribution of the refractive index. The general idea is to produce a fringe pattern modulated by the variations in refractive index. Mathematically, the intensity of an interferogram can be

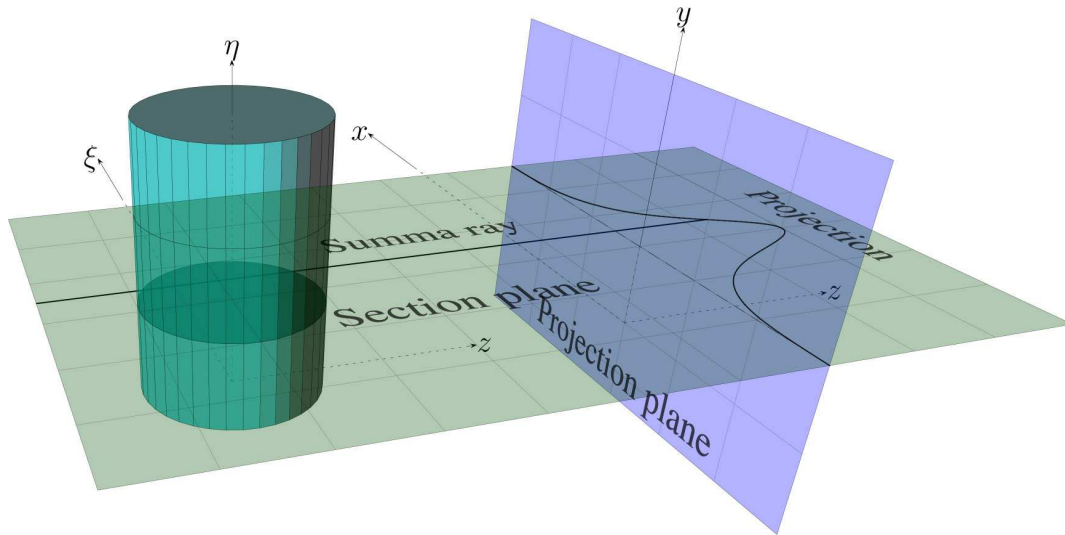


FIG. 1 Graphical description of a projection of a phase object section.

represented as:

$$I(x, y) = a(x, y) + b(x, y) \cos[2\pi f_0 x + \phi(x, y)] \otimes \eta(x, y), \quad (1)$$

Where (x, y) are the spatial coordinates, $a(x, y)$ represents the background light, $b(x, y)$ is the modulation in amplitude and $\phi(x, y)$ the phase of the wavefront associated to the refractive index; f_0 is the frequency of the carrier [8] and $\eta(x, y)$ represents the noise. The symbol \otimes indicates that noise can be either additive or multiplicative since, in the case of Speckle Pattern Interferometry (SPI) [5] or single path interferometry [1], noise is multiplicative. When the level of noise is significant, it is necessary to employ some filtering method. In many practical cases, and for the purposes of this work, both a and b vary slowly. If the interferogram does not have a carrier, i.e., ($f_0 = 0$), as that from a single path interferometer and from the holographic ones [1] the fringe pattern can be described by:

$$I(x, y) = \cos[\phi(x, y)] \eta(x, y). \quad (2)$$

As for the tomographic reconstruction, let us consider that the optical path length δ of a single ray, across a transparent medium, is represented as:

$$\delta = \int_C n ds, \quad (3)$$

which is the integral of the refractive index n along the path of the ray C . When the refraction is not intense, the path of the ray can be approximated by a straight line. If the ray propagates along the z axis, as illustrated in Figure 2, the optical path can be thus expressed as:

$$\delta(\xi, \eta) = \int_C n(\xi, \eta) dz, \quad (4)$$

and the optical path difference (OPD) $\Delta(\xi, \eta)$ is given as

$$\Delta(\xi, \eta) = \int [n(\xi, \eta) - n_0] dz, \quad (5)$$

where n_0 is the refractive index of the surrounding medium and $\Delta(x, y)$ is related to the phase of $\phi(x, y)$, in Eq. (2), as:

$$\phi(x, y) = \frac{2\pi}{\lambda} \Delta(\xi, \eta). \quad (6)$$

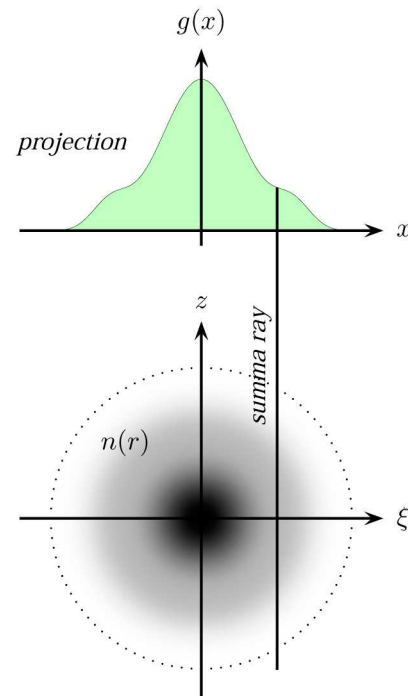


FIG. 2 The Abel Transform applied on a section of a phase object.

In the particular case of a radially-symmetrical PO and by considering a section of it (as illustrated in Figure 2), Eq. (3) can be expressed in terms of the Abel transform, $\mathcal{A}\{\cdot\}$ [1], as:

$$\Delta(\xi) = \Delta(\xi, \eta = cte) = \mathcal{A}\{n(r)\} = 2 \int_{\xi}^{+\infty} \frac{n(r) r}{\sqrt{r^2 - \xi^2}} dr, \quad (7)$$

where r is the radial coordinate given by $\sqrt{\xi^2 + \eta^2}$.

3 ALTERNATIVE RECONSTRUCTION METHOD

As it is well known, in the ART methods, the cross section of the object is superimposed onto a logic grid of $M \times N$ elements [3]. Each of these elements or pixels is an unknown

[2]–[5], [9, 10]. To describe each pixel, different definitions are used, e. g. rectangles or some other local function that can overlap with neighboring elements [9, 10]. To reconstruct the section, at least, $M \times N$ equations should be set. The methods available in the specialized literature are rather general and not oriented to a specific distribution. For radially symmetrical objects, the generator function is divided into M elements. To reconstruct the section, at least M equations are necessary in order to know these elements of the generator function. Fortunately, it is possible to simplify the problem by considering only smooth radially symmetric PO [6]. This assumption allows for a rapid reconstruction of the cross section, considering only representative points of the interferogram. These points are obtained from the contour curves built from the interferogram, without a carrier.

Indeed, provided the PO is mathematically smooth and continuous, it is assumed that the profile of a section, $n(r)$, can be approximated by a linear combination of k non-local Gaussian basis functions $f_i(r)$, i.e.

$$n(r) \approx \sum_{i=1}^k w_i f_i(r), \tag{8}$$

here w_i are weighting factors. From Eqs. (6), (7) and (8) the optical path difference is

$$\begin{aligned} N(x) \lambda &= \mathcal{A} \left\{ \sum_{i=1}^k w_i f_i(r) \right\} = \sum_{i=1}^k w_i \mathcal{A} \{ f_i(r) \} \\ &= \sum_{i=1}^k w_i F_i(x), \end{aligned} \tag{9}$$

where $N(x)$ is the optical path difference in magnitude and $F_i(x)$ is the Abel transform of the basis function $f_i(r)$. If x lies within the range $0 \leq x \leq x_m$, where x_m is the maximum value of x , then Eq. (9) can be expressed in matrix form as

$$\begin{pmatrix} F_1(x_1) & F_2(x_1) & \cdots & F_k(x_1) \\ F_1(x_2) & F_2(x_2) & \cdots & F_k(x_2) \\ \vdots & \vdots & & \vdots \\ F_1(x_n) & F_2(x_n) & \cdots & F_k(x_n) \\ F_1(x_m) & F_2(x_m) & \cdots & F_k(x_m) \end{pmatrix} \begin{pmatrix} w_1 \\ w_2 \\ \vdots \\ w_k \end{pmatrix} = \lambda \begin{pmatrix} N_1 \\ N_2 \\ \vdots \\ N_n \\ N_m = 0 \end{pmatrix}, \tag{10}$$

where x_1, x_2, \dots, x_n are the central positions of the orders N_1, N_2, \dots, N_n for a given value of y . Position x_m is assigned to the m th (N_m), which corresponds to the surrounding. Then, the Eq. (10) can be expressed as

$$\boldsymbol{\varphi} = \lambda \mathbf{N} = \mathbf{F} \mathbf{w} \tag{11}$$

with \mathbf{N} being the vector that contains the orders of interferogram, \mathbf{w} as the vector of weights of the contributions of the functions $F_i(x)$ and \mathbf{F} is the projection matrix. The mean square error (MSE) is given by

$$MSE = \frac{1}{MN} \mathbf{E}^T \mathbf{E} = \frac{1}{MN} (\boldsymbol{\varphi} - \mathbf{F} \mathbf{w})^T (\boldsymbol{\varphi} - \mathbf{F} \mathbf{w}). \tag{12}$$

By differentiating the last expression with respect to \mathbf{w} and making it equal to zero, one obtains,

$$\mathbf{w} = \left(\mathbf{F}^T \mathbf{F} \right)^{-1} \mathbf{F}^T \boldsymbol{\varphi}, \tag{13}$$

where the matrix $(\mathbf{F}^T \mathbf{F})^{-1} \mathbf{F}^T$ is the pseudo inverse of \mathbf{F} . Therefore, to obtain an estimate $n(r)$ it is only required to calculate the weights w_i , from Eq. (9). For the pseudo inverse of \mathbf{F} the methods described in the literature [11, 12] can be used. The pseudo inverse can also be calculated using commercial software such as MATLAB[®] or MathCad[®]. In summary, given a set of non-local Gaussian basis functions, the alternative method proposed consists in finding the linear combination of this set that best fits the vector \mathbf{N} .

The specific steps for the application of this method can be described in the next sequence:

1. Eliminate the noise.
2. Obtain the central positions of the orders (x_1, x_2, \dots, x_n).
3. Acquire the contour curves (N_1, N_2, \dots, N_n).
4. Set the refractive index of PO.
5. Associate the refractive index with a physical quantity.

4 RESULTS AND DISCUSSION

The simplest approach for tomographic reconstruction of a PO section consists in a linear approximation of rings of width Δr of such section [1]. Given this approximation Eq. (9) can be expressed as

$$N_i \lambda = 2 \sum_{k=1}^{I-1} f_k \int_{r_k}^{r_{k+1}} \frac{r}{(r^2 - r_i^2)^{1/2}} dr, \tag{14}$$

By solving the integral we obtain

$$\sum_{k=i}^{I-1} A_{ik} f_k = \left(\frac{\lambda}{2\Delta r} \right) N_i, \tag{15}$$

where $A_{ik} = \left\{ \left[(k+1)^2 - i^2 \right]^{1/2} - \left[k^2 - i^2 \right]^{1/2} \right\}$.

Finally, Eq. (15) can be expressed as

$$\begin{pmatrix} A_{11} & A_{12} & \cdots & A_{1k} \\ 0 & A_{22} & \cdots & A_{2k} \\ \vdots & \vdots & & \vdots \\ 0 & 0 & \cdots & A_{ik} \end{pmatrix} \begin{pmatrix} f_1 \\ f_2 \\ \vdots \\ f_k \end{pmatrix} = \frac{\lambda}{2\Delta r} \begin{pmatrix} N_1 \\ N_2 \\ \vdots \\ N_i \end{pmatrix}. \tag{16}$$

In order to find the vector \mathbf{f} , a total of $(I-1)^2$ operations are required, where I is the number of rings. For the reconstruction of PO an overall of $(I-1)^2 \times n_s$ operations are required, with n_s is the number of sections.

On the other hand, to find the weights of the basis functions in the proposed method, $3n_p^3 n_f$ operations are required, where n_p is the number of points corresponding to the orders of the

interferogram, and n_f is the number of basis functions. For the PO reconstruction $2n_p n_f n_s$ operations are required. Therefore, the total number of operations is $3n_p^3 n_f + 2n_p n_f n_s$

To assess the quality of the reconstruction, a numerical simulation was performed as follows. A wavefront is projected through a radial symmetrical PO $n_t(r, n)$, given by the equation

$$n_t(r, \eta) = -10.5 \times 10^{-5} \left[\exp(-5x^2) + \exp\left(-\frac{5}{9}x^2\right) \right], \quad (17)$$

where $r = \sqrt{\xi^2 + \eta^2}$ is given in *cm*. Figure 3 shows one projection section of PO (OPD in λ) and the corresponding interferogram (for $\lambda = 632.8$ nm, HeNe laser). From each order's centers, the level points shown as the neighbor of the OPD are obtained. The total set of level points, 23 points, are used to obtain an approximation of the PO section. Figure 4 shows the reconstructions obtained using five and seven uniformly

distributed gaussians, in two intervals, with a separation between centers of σ units.

For the reconstruction, rings with a Gaussian profile are used

$$gauss(r - r_0, \sigma) = \exp\left[-\frac{(r - r_0)^2}{2\sigma^2}\right], \quad (18)$$

where σ is given by

$$\sigma = \frac{x_m}{(n_g - 1)d}. \quad (19)$$

being n_g the number of Gaussians used in the reconstruction and d the distance between their centers, measured in σ .

From the points shown in Figure 3, the reconstruction is shown in Figure 4, with 5 Gaussian functions and separation between their centers σ .

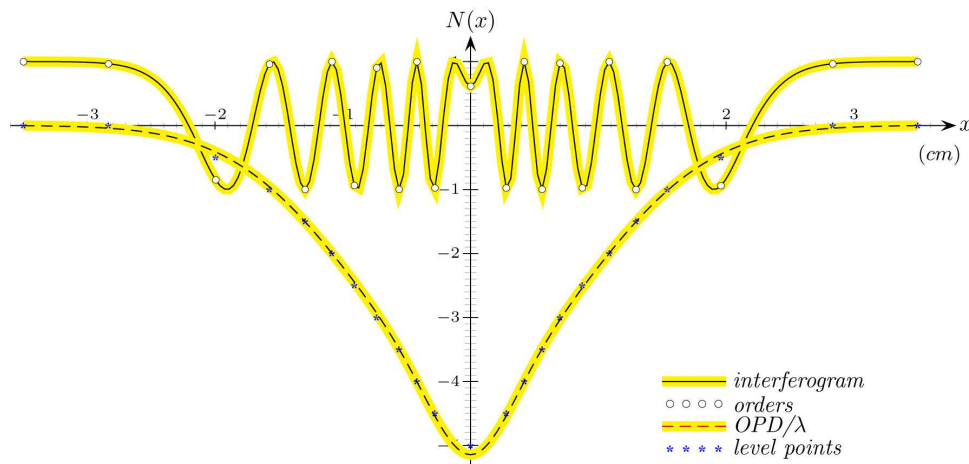


FIG. 3 Interferogram and OPD from PO.

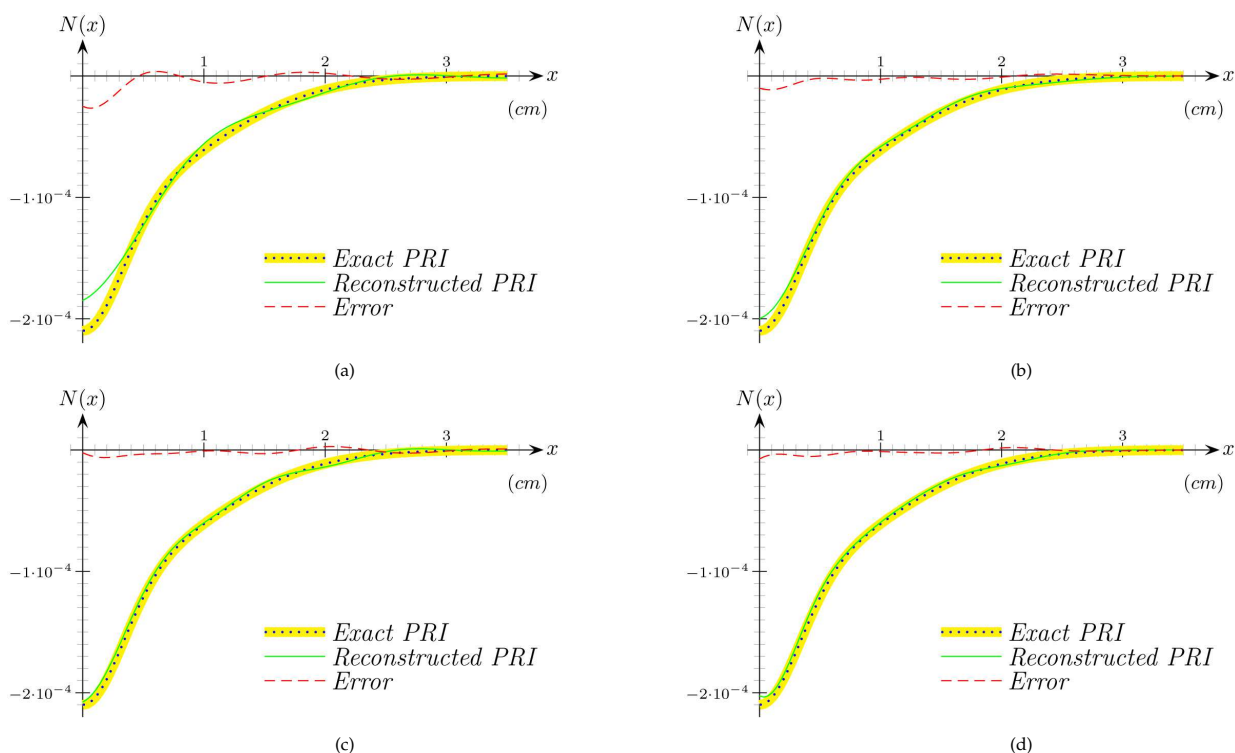
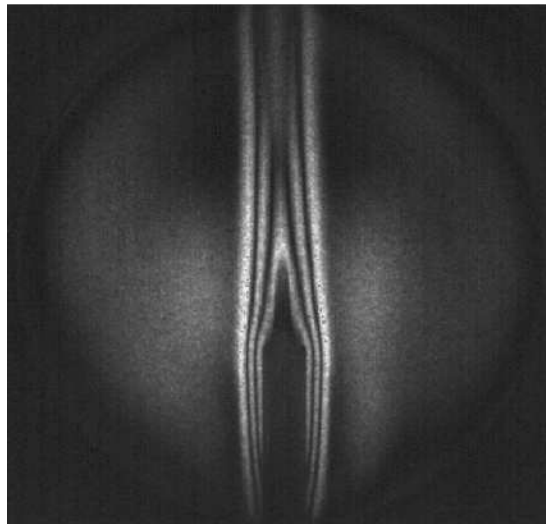


FIG. 4 Reconstruction of a section of the object, using our proposed technique. (a) five Gaussians, $[0, 2.85]$. (b) five Gaussians, $[0, 2]$. (c) seven Gaussians, $[0, 2.85]$. (d) seven Gaussians, $[0, 2]$.



(a) The complete interferogram



(b) The region of interest of in the Figure 5a.

FIG. 5 Interferograms from hot tip

As an actual real example of our approach, Figure 5(a) shows the experimental interferogram for the hot tip obtained by means of an in-axis interferometer in a non-linear medium. The experimental details were published separately [13]. Figure 5(b) corresponds to a selected region of the original interferogram, filtered to eliminate the noise (a Wiener filter [1, 5] with a window of 3×41 was employed). By using $\lambda = 632.8$ nm, a distance between two adjacent elements of $\Delta\xi = \xi_i - \xi_{i-1} = 0.0333$ cm and a linear combination of four rings of a gaussian profile, the curves of Figure 6(a) are obtained. The Gaussians are uniformly distributed in $[0, L(3)]$ (where $L(3)$ is the maximum value of the third order, from right to left from each PO section).

The latter are associated with temperature gradients through the Gladstone-Dale equation [1].

$$n - 1 = \frac{0.292015 \times 10^{-3}}{1 + 0.368184 \times 10^{-2}T}, \quad (20)$$

where n is the refractive index and T is temperature in $^{\circ}\text{C}$. In Figure 6(b) a longitudinal slice is shown. Figure 6(c) shows three transversal slices of the PO's temperatures. As summary, Figure 6(d) shows a 3D view.

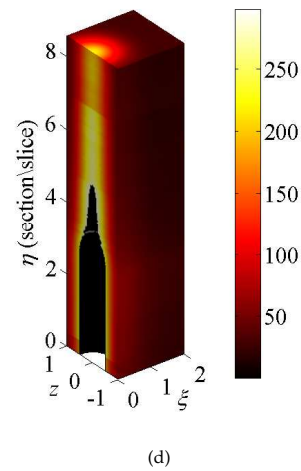
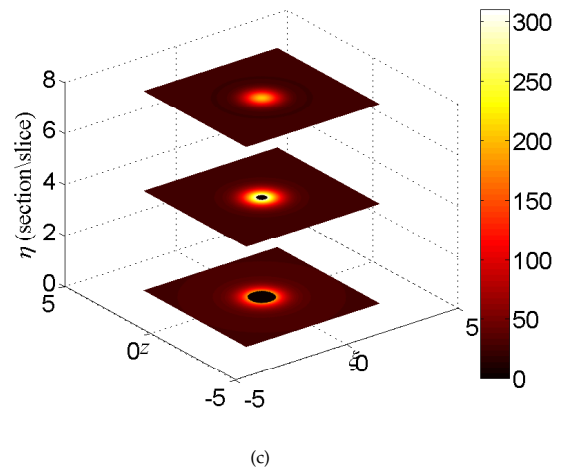
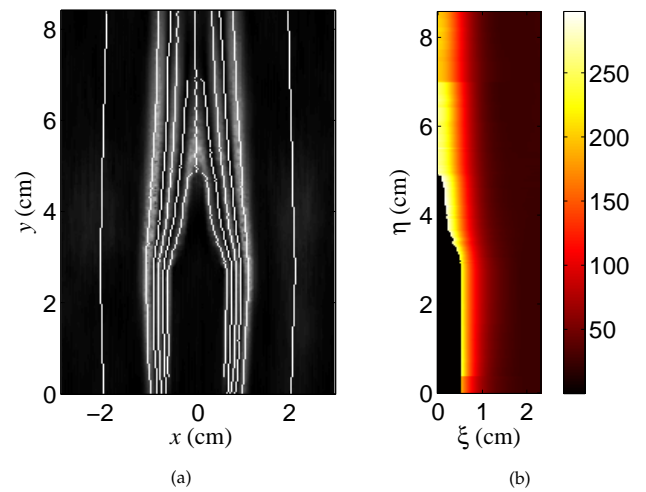


FIG. 6 (a) Level fringes of the PO. (b) Longitudinal slice, (c) transversal slices, and (d) 3D view, of the PO's temperature.

5 CONCLUSION

The proposed method is a simple algebraic, fast and accurate non-iterative algorithm. It is fast because the number of unknowns (the weights of basis functions) is small. And it is accurate because the reconstruction can be done on representative points from the orders of the detected interferogram. Moreover, this approach can be improved further by using an interpolation according to the symmetry and the type of object, resulting in a more accurate reconstruction, at will.

ACKNOWLEDGEMENTS

We want to thank the *Universidad Autónoma de Zacatecas*, the *National Institute of Astrophysics, Optics and Electronics*, and FOMIX ZAC-2011-C01-172823 for all the support for this work. We are also grateful to the authors of reference [13] for the interferogram of the hot tip,

References

- [1] C. M. Vest, *Holographic Interferometry* (John Wiley & Sons, New York, 1979).
- [2] S. R. Deans, *The Radon Transform, and Some of its Applications* (First edition, Wiley, New York, 1983).
- [3] R. M. Lewitt, "Reconstruction Algorithms: Transform Methods," *Proc. IEEE* **71**, 390-408 (1983).
- [4] H. J. Scudder, "Introduction to Aided Tomography," *Proc. IEEE* **66**, 628-637 (1978).
- [5] A. K. Jain, *Fundamentals of Digital Image Processing* (Prentice Hall, New Jersey, 1989).
- [6] V. Dribinski, A. Ossadtchi, V. A. Mandelshtam, and H. Reisler, "Reconstruction of Abel-transformable images: The Gaussian basis-set expansion Abel transform method," *Rev. Sci. Instrum.* **73**, 2634-2642 (2002).
- [7] K. J. Gasvik, *Optical Metrology* (Wiley, New York, 1987).
- [8] M. Takeda, H. Ina, and S. Kobayashi, "Fourier-Transform Method of Fringe-Pattern Analysis for Computer-Based Topography and Interferometry," *J. Opt. Soc. Am. A* **72**, 156-160 (1981).
- [9] K. M. Hanson, and G. W. Wecksung, "Local Basis-Function Approach to Computed Tomography," *Appl. Opt.* **24**, 4028-4039 (1985).
- [10] Y. Censor, "Finite Series-Expansion Reconstruction Methods," *Proc. IEEE* **71**, 409-419 (1983).
- [11] G. H. Golub, and C. F. Van Loan, *Matrix Computations* (Third edition, The John Hopkins University Press, Baltimore, 1996).
- [12] W. H. Press, S. A. Teukolsky, W. T. Vetterling, and B. P. Flannery, *Numerical Recipes in C: The Art of Scientific Computing* Second edition, Cambridge University Press, New York, 1992).
- [13] C. G. Treviño-Palacios, M. D. Iturbe-Castillo, D. Sánchez-de-la-Llave, R. Ramos-García, and L. I. Olivos-Pérez, "Nonlinear comon-path interferometer: An image processor," *Appl. Opt.* **42**, 5091-5095 (2003).